

Mass Assembly of High-z Galaxies with MASSIV

V. Perret*, B. Epinat, P. Amram, O. Le Fèvre, C. Lopez-Sanjuan, L. Tasca, L. Tresse

*Aix Marseille Université, CNRS, LAM (Laboratoire d'Astrophysique de Marseille) UMR 7326,
13388, Marseille, France*

E-mail: valentin.perret@oamp.fr

T. Contini, C. Divoy, J. Queyrel, J. Moutaka

IRAP, Université de Toulouse, UPS-OMP, CNRS, Toulouse, France

D. Vergani

INAF IASFBO, Via P. Gobetti 101, I-40129 Bologna, Italy

F. Bournaud

CEA, IRFU, SAp, F-91191 Gif-sur-Yvette, France

B. Garilli, L. Paoro

INAF-IASFMI, Via E. Bassini 15, I-20133 Milano, Italy

M. Kissler-Patig

ESO, Karl-Schwarzschild-Str. 2, D-85748 Garching b. München, Germany

MASSIV (Mass Assembly Survey with SINFONI in VVDS) is a sample of 84 distant star-forming galaxies observed with the SINFONI Integral Field Unit (IFU) on the VLT. These galaxies are selected inside a redshift range of $0.8 < z < 1.9$, i.e. where they are between 3 and 5 billion years old. The sample aims to probe the dynamical and chemical abundances properties of representative galaxies of this cosmological era. On the one hand, close environment study shows that about a third of the sample is involved in major mergers. On the other hand, kinematical analysis revealed that 42% of the sample is rotating disks, in accordance with higher redshift samples. The remaining 58% show complex kinematics, suggesting a dynamical support based on dispersion, and about half of these galaxies is involved in major mergers. Spheroids, unrelaxed merger remnants, or extremely turbulent disks might be an explanation for such a behavior. Furthermore, the spatially resolved metallicity analysis reveals positive gradients, adding a piece to the puzzle of galaxies evolution scenarios.

VIII International Workshop on the Dark Side of the Universe,

June 10-15, 2012

Rio de Janeiro, Brazil

*Speaker.

1. Mass Assembly of High Redshift Galaxies

In the current framework of Λ CDM cosmology, the mean energy density of the Universe is shared between dark energy, dark matter and baryonic matter. In this context, the formation of structures in the Universe is seeded by small perturbations in matter density expanded to cosmological scales by inflation. Given such a cosmological model, the Universe is about 13.7 billion years old, and galaxies are expected to form around $z=20-50$ (Gao et al. 2007), when the first sufficiently deep dark matter potential wells are made and allowed gas to cool and condense to produce primeval stars and galaxies.

This standard model reproduces well the linear initial conditions, the intergalactic medium structure during galaxy formation, and large scale structure as observed today. However, the hierarchical dark matter halo formation paradigm remains strongly debated. The physical processes responsible for mass assembly at early epochs is still unclear. While merging events are expected to play an important role in the building of the Hubble sequence, smooth cold gas accretion might also have strongly contributed to the growth of galaxies. Secular processes such as stellar feedback may also have a major role in the build-up of local galaxies. High- z galaxies tend to have a higher gas fraction, thus a powerful stellar feedback would be able to drive the evolution within the gravitational potential.

This debate can be addressed with spatially resolved measurements from 3D spectral analysis, allowing to probe various physical quantities, e.g. star formation, gas kinematics, chemical abundances. The MASSIV sample investigates a redshift range unexplored by Integral Field Spectroscopy (IFS), considering that four distinct 3D surveys are preceding it. IMAGES (Puech et al. 2008) sample, with $0.4 < z < 0.75$, showed that regular rotating disks are quite similar to the local ones and that mergers are playing an important role in galaxy mass assembly. SINS (Förster Schreiber et al. 2009) sample, Wright et al. (2009) and Law et al. (2009) samples, and LSD/AMAZE (Maiolino et al. 2008) sample, with $z > 1.5$ (mostly with $z > 2$), showed that a lot of young galaxies are experiencing a high gaseous turbulence.

The MASSIV sample was built to probe representative galaxies in the redshift range $0.8 < z$

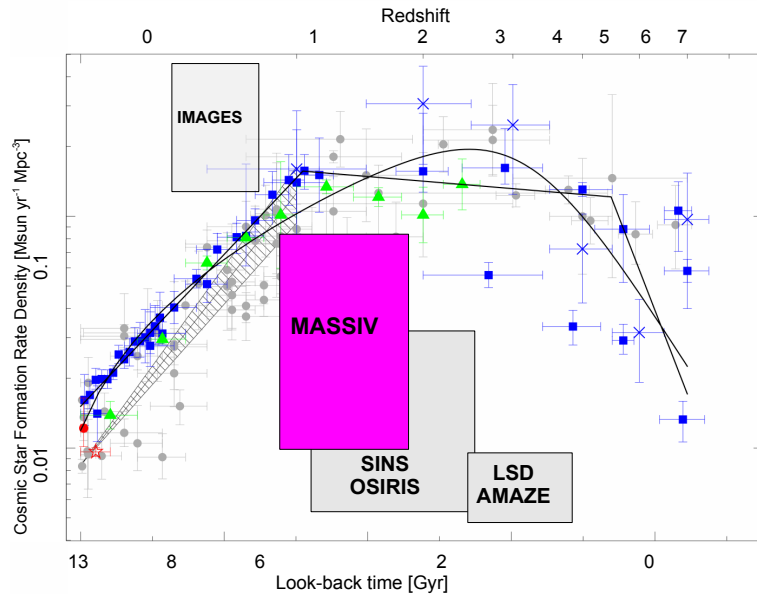


Figure 1: Evolution of the cosmic star formation rate density as a function of look-back time and redshift. Major IFU surveys redshift ranges are compared. The relative height of each box is proportional to the sample size. Adapted from Contini et al. (2012).

< 1.9 (Fig. 1), where the cosmic star formation rate history is expected to peak (Cucciati et al. 2012), and where we look forward to a transition between small and disturbed galaxies towards the Hubble sequence. This redshift range is also an opportunity to infer the establishment of the stark dichotomy within the galaxy population, already in place at $z=1$.

MASSIV is an ESO large program (200 hours) grouping 84 galaxies observed with the NIR-IFU SINFONI on the VLT from 2008 until completion in 2011 (Contini et al. 2012). The J- or H-bands have been used to target the redshifted $H\alpha$ emission line with a high spatial resolution ($< 0.8''$), and a total integration time varying between 80 and 120 min. Among these 84 galaxies, 11 were observed with the adaptive optics system (AO), reaching a spatial resolutions close to $0.20''$. As of today, it is the largest sample of high- z galaxies observed with IFS.

The strength of this survey lies in its well defined parent sample, that is the VVDS (Le Fèvre et al. 2005) a redshift survey selected in magnitude ($I_{AB} \leq 24$) including 35000 spectra in the visible, avoiding any biases linked to a priori color selection techniques. A high completeness of the parent sample is mandatory if one wants to probe normal and representative galaxies. Galaxies were selected on [OII]3727 equivalent width strength or rest-frame UV intensity from SED fitting, both being a proxy for star formation. This star formation criterion ensures that the brightest rest-frame optical emission line $H\alpha$ ([OIII]5007 for a few galaxies) is available to probe resolved kinematics and chemical abundances down to galaxies with a SFR close to $1 M_{\odot} \text{yr}^{-1}$. Galaxies were selected to have a sufficiently close bright star valuable for AO/LGS. The continuum I-band magnitude of each galaxy is estimated using the best-seeing CFHT-LS images with a resolution better than $0.65''$.

Fig. 2 compares the relation between stellar mass and star formation rate for the major IFU samples, over-plotting empirical relations for different redshifts. On the one hand, we see that for a given stellar mass SINS, LSD/AMAZE are globally probing galaxies with higher star formation rate than MASSIV, while on the other hand, for a given stellar mass, the IMAGES sample is globally probing galaxies with a lower star formation rate than what is expected for a representative sample.

2. Kinematical analysis of MASSIV galaxies

The full MASSIV sample allows resolved velocity measurement for $\sim 90\%$ of the galaxies. Each velocity field was fitted using a PSF-convolved 'flat' model rotation curve (Epinat et al. 2010).

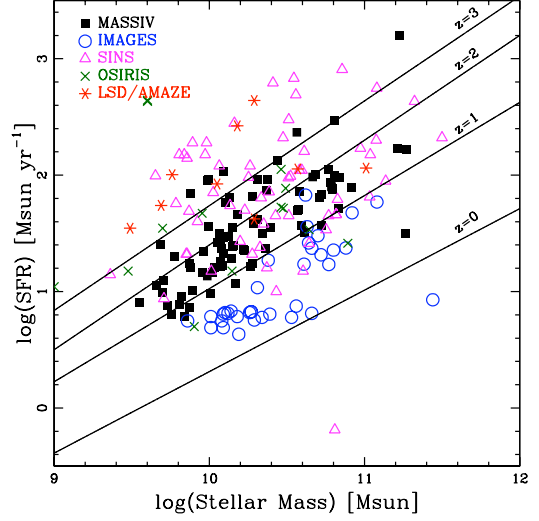


Figure 2: SED-derived star formation rate as a function of stellar mass. The lines represent the empirical relations between SFR and stellar mass for different redshifts between $z = 0$ and $z = 3$ following the analytical expression given in Bouché et al. (2010). All the illustrated IFU samples are rescaled to match the MASSIV sample redshift range. Adapted from Contini et al. (2012).

A kinematical classification of the first epoch sample has been performed in Epinat et al. (2012), using three distinct estimators. A first parameter used to distinguish fast rotators from slow rotators is the total velocity shear V_{shear} measured on the velocity field, without any inclination correction (see Fig. 3). With this simple parameter applied on the full sample, 33 (42%) galaxies exhibit high velocity shear ($V_{shear} > 100 \text{ km.s}^{-1}$), and 45 (58%) galaxies have a low velocity shear ($V_{shear} < 100 \text{ km.s}^{-1}$).

We also compared a parameter measuring the discrepancy between the position angle of the major axis (PA) of the stellar component and the kinematical PA of the gaseous component with the mean weighted velocity field residuals normalized by the velocity shear. Similarly it gives 33 (42%) galaxies classified as "rotating", and 45 (58%) galaxies classified as "non-rotating" systems.

In addition, the immediate environment of each galaxy is probed to determine whether the galaxy lies isolated or not. We search for companions in both the $H\alpha$ and I-band image, with a relative velocity lower than 1000 km.s^{-1} and a projected distance lower than $50 h^{-1}.kpc$. Applying this method, 59 (76%) galaxies are found to be isolated, and 19 (24%) are not.

This work on close environ-

ment has been pushed further away by López-Sanjuan et al. (2012). Defining a close pair as a couple of galaxies with a projected radial separation lower than $20 h^{-1}.kpc$, and a radial velocity difference lower than 500 km.s^{-1} , we are able to recover a major merger rate $R_{MM} \propto (1+z)^{3.95}$ in the MASSIV redshift range.

Although the origin of galaxies with high V_{shear} is clear (disks with ordered rotation), galaxies with low V_{shear} are more difficult to interpret. Face-on disks, unrelaxed merger remnants, or star-forming spheroids could be an explanation to such a behavior. Nevertheless, the orientation of disks with spin vectors randomly distributed could only account for 14% of this low-shear population considering disks rotating at $V_{rot}=200 \text{ km.s}^{-1}$. The large fraction of interacting, and non-rotating galaxies seems to suggest that an important cosmological mass assembly mechanism is at work between redshift 1 and 2.

3. Fundamental relations with MASSIV

In Vergani et al. (2012) we investigate the fundamental relations using MASSIV data. With dynamical arguments, we derive a gas mass that is on average a fraction of $\sim 45\%$ of the dynamical mass, assuming no central contribution of dark matter, as in Gnerucci et al. (2011), and consistent with lower concentration parameter of haloes at high- z (Bullock et al. 2001). This gas content is consistent with the fraction derived using the Kennicutt-Schmidt formulation.

The evolution of the Tully-Fischer Relation (TFR) is expected to be related both to the conversion of gas into stars and to the inside-out growth of dark matter halo by accretion. In Vergani

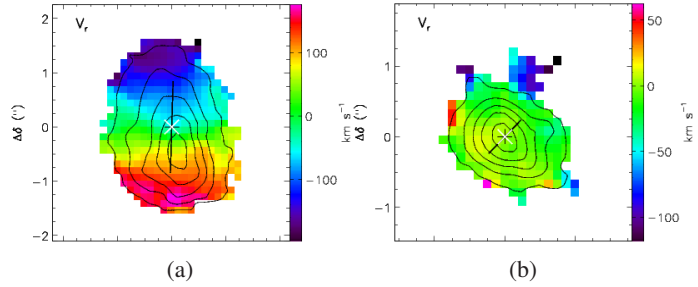


Figure 3: (a) High-shear velocity field (VVDS220584167). (b) Low-shear velocity field (VVDS020386743). Contours are drawing the $H\alpha$ flux distribution. Adapted from Epinat et al. (2012).

et al. (2012) the stellar mass TFR shows a negligible, net evolution in the past 8 Gyrs with a large scatter that is reduced, but still remarkable, using the S_{05} index ($S_{05} = \sqrt{0.5 \times v_{rot}^2 + \sigma_0^2}$, Fig. 4). We interpret this behavior as an evidence of complex physical mechanism(s) at work in our stellar mass/luminosity regime and redshift range. We also conclude a marginal evolution in the size - stellar mass and size - velocity relations in which disks become evenly smaller with cosmic time at fixed stellar mass or velocity, and are less massive at a given velocity than in the local Universe in agreement with cosmological hydrodynamical simulations, e.g. Portinari & Sommer-Larsen (2007).

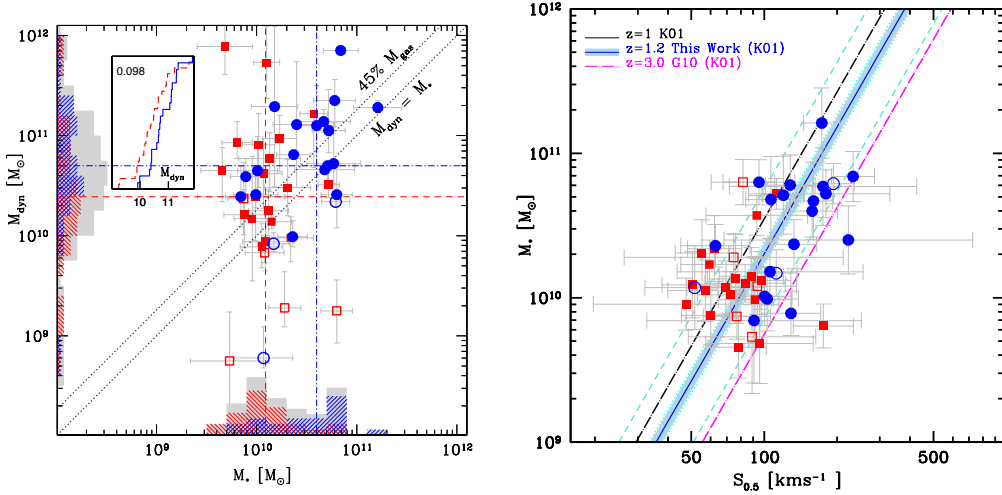


Figure 4: **Left:** Stellar mass content of the MASSIV galaxies compared to the dynamical modeling M_{dyn} . The blue/red points corresponds to rotating/non-rotating galaxies according to Epinat et al. (2012) criterion. The empty, dashed symbols show galaxies detected with a low signal-to-noise ratio ($3 \leq \text{SNR} \leq 4.5$). The horizontal and vertical lines are the median values of rotators (point-dashed blue line) and non-rotators (dashed red line). The relation $M_{dyn} = M_{\star} + M_{gas}$ is over-plotted with the mean value of the gas fraction (45%) for both rotators and non-rotators. **Right:** Stellar mass TFR at $z \sim 1.2$ (blue line) based on rotating MASSIV galaxies (blue dots), taking into account both the ordered and chaotic motions (Kassin et al. 2001, K01). We over-plot the $z \sim 1$ slope by Kassin et al. (2007) (solid black line), and the $z \sim 3$ slope by Gnerucci et al. (2011) (long-dashed magenta line). The cyan shaded area shows the 1σ error on the zero-point parameter, the cyan dotted line and cyan dashed line are the intrinsic and total scatter, respectively. Adapted from Vergani et al. (2012).

4. Abundance gradients with MASSIV

The first epoch sample (50 galaxies) enabled an abundances analysis in Queyrel et al. (2012). The metallicity of galaxies was derived in taking the $[\text{NII}]/\text{H}\alpha$ ratio, with the Pérez-Montero & Contini (2009) calibration. Among these 50 galaxies, 26 metallicity gradients were measured inside spatially distinct annular regions defined by the $\text{H}\alpha$ contour map. While half of the sample (14 galaxies) is compatible with a zero metallicity gradient, a quarter (7 galaxies) of the restricted

sample exhibits positive metallicity gradients. Among these positive gradients, 4 are classified as interacting systems, one might be a chain galaxy, and 2 are flagged as isolated. Such features have been observed in local interacting galaxies (Werk et al. 2010); it would be an effect of a fresh metal-poor gas infall onto the core of the merger remnant.

The isolated galaxies detected with positive gradients are more puzzling objects. Such systems have been observed in Cresci et al. (2009), suggesting that cold gas accretion onto the center of the central regions would be a plausible scenario. The radial abundances of the second epoch sample will be published soon, and they will extend the statistics of this first analysis.

5. Simulations

High redshift disks have been performed in numerical simulations by Bournaud et al. (2011) who have shown that the input of large gas fraction (40-60%) in the initial conditions led to chaotic and turbulent gaseous disks. Among different question to tackle in the near future, the understanding of the underlying processes responsible for the non-rotating galaxies in the redshift range $0.8 < z < 1.9$ led us to simulate high redshift disks from idealized mergers. We are sampling different orbital parameters and mass ratio through a set of 20 simulations. These simulations will be projected on the sky plane at different evolutionary time using numerous projection angles to mimic observational configurations. Using the RAMSES code (Teyssier 2002), we are producing simulations of mergers with a physical resolution reaching 6 pc, coupled with a new implementation handling the feedback of OB-type stars emitting energetic ultraviolet photons. With this data we aim to disentangle the different scenarios leading to the formation of a population of galaxies with a low V_{shear} , as well as the conditions required for the disk survival.

References

- Bouché, N., Dekel, A., Genzel, R., et al. 2010, ApJ, 718, 1001
- Bournaud, F., Chapon, D., Teyssier, R., et al. 2011, ApJ, 730, 4
- Bullock, J. S., Kolatt, T. S., Sigad, Y., et al. 2001, MNRAS, 321, 559
- Contini, T., Garilli, B., Le Fèvre, O., et al. 2012, A&A, 539, A91
- Cresci, G., Hicks, E. K. S., Genzel, R., et al. 2009, ApJ, 697, 115
- Cucciati, O., Tresse, L., Ilbert, O., et al. 2012, A&A, 539, A31
- Epinat, B., Amram, P., Balkowski, C., & Marcelin, M. 2010, MNRAS, 401, 2113
- Epinat, B., Tasca, L., Amram, P., et al. 2012, A&A, 539, A92
- Förster Schreiber, N. M., Genzel, R., Bouché, N., et al. 2009, ApJ, 706, 1364
- Gao, L., Yoshida, N., Abel, T., et al. 2007, MNRAS, 378, 449

- Gnerucci, A., Marconi, A., Cresci, G., et al. 2011, *A&A*, 528, A88
- Kassin, S. A., Weiner, B. J., Faber, S. M., et al. 2007, *ApJ*, 660, L35
- Law, D. R., Steidel, C. C., Erb, D. K., et al. 2009, *ApJ*, 697, 2057
- Le Fèvre, O., Vettolani, G., Garilli, B., et al. 2005, *A&A*, 439, 845
- López-Sanjuan, C., Le Fèvre, O., Tasca, L. A. M., et al. 2012, *ArXiv e-prints*
- Maiolino, R., Nagao, T., Grazian, A., et al. 2008, *A&A*, 488, 463
- Pérez-Montero, E. & Contini, T. 2009, *MNRAS*, 398, 949
- Portinari, L. & Sommer-Larsen, J. 2007, *MNRAS*, 375, 913
- Puech, M., Flores, H., Hammer, F., et al. 2008, *A&A*, 484, 173
- Queyrel, J., Contini, T., Kissler-Patig, M., et al. 2012, *A&A*, 539, A93
- Teyssier, R. 2002, *A&A*, 385, 337
- Vergani, D., Epinat, B., Contini, T., et al. 2012, *A&A*, 546, A118
- Werk, J. K., Putman, M. E., Meurer, G. R., et al. 2010, *ApJ*, 715, 656
- Wright, S. A., Larkin, J. E., Law, D. R., et al. 2009, *ApJ*, 699, 421